Supplementary information: Revealing the Role of Redox Reaction Selectivity and Mass Transfer in Current–Voltage Predictions for Ensembles of Photocatalysts

Luisa Barrera[1,2], Bradley W. Layne[3], Zejie Chen[3], Kenta Watanabe[5,6], Akihiko Kudo[5], Daniel V. Esposito[4], Shane Ardo[3,7,8], Rohini Bala Chandran[1,*]

[1] Department of Mechanical Engineering, University of Michigan, Ann Arbor, MI 48109
[2] *current institution*, School of Mechanical Engineering, Georgia Institute of Technology, Atlanta, GA 30308
[3] Department of Chemistry, University of California Irvine, Irvine, CA 92697
[4] Department of Chemical Engineering, Columbia University, New York, NY
[5] Department of Applied Chemistry, Faculty of Science, Tokyo University of Science, Tokyo 162-8601, Japan
[7] Departments of Chemical & Biomolecular Engineering, University of California Irvine, Irvine, CA 92697
[8] Department of Materials Science and Engineering, University of California Irvine, Irvine, CA 92697

**Corresponding author, rbchan@umich.edu*

Nomenclature

Symbols	
A	absorptance, dimensionless
A_c	area of the light absorber, m^2
c	speed of light, 3×10^8 m s^{-1}
C	mass concentration of particles, mg mL^{-1}
E_{bg}	bandgap of photodiode, 1.55 eV
E_{eq}	Nernst potential for redox reaction, V *vs* NHE
F	Faraday constant, 96500 C mol^{-1}
$\Delta g^0_{\mathrm{net}}$	standard Gibbs free energy difference associated with a redox reaction pair, kJ mol^{-1}
h	Planck constant, $6.62607004 \times 10^{-34}$ m^2 kg s^{-1}
j	current density, A m^{-2}
j_0	exchange current density, A m^{-2}
k_B	Boltzmann constant, 1.380649×10^{-23} J K^{-1}
n	spatial position of light absorbers with respect to the top of the ensemble of light absorbers, dimensionless
n_e	number of electrons, dimensionless
N	number of light absorbers, dimensionless
q_e	elementary charge, $1.60217662 \times 10^{-19}$ C
R	gas constant, 8.314 J mol^{-1} K^{-1}
S_{rxn}	reaction selectivity at each photodiode band, dimensionless
T	ambient temperature of the system and surroundings, 298.15 K
V_{op}	operating potential of the photodiode, V
V_{oc}	open-circuit potential of the photodiode, V

Greek	
α	charge-transfer coefficient, dimensionless
η	overpotential, V
υ	photon frequency, s^{-1}

ν	stoichiometric coefficient for reactions, dimensionless
ρ	bulk density of material, g cm^{-3}
τ	optical thickness, dimensionless
ϕ_{solar}	frequency-dependent incident photon flux, s^{-1} m^{-2}

Subscripts	
a	pertinent to the anodic reaction
b	pertinent to the semiconductor conduction or valence band b
bg	pertinent to the bandgap
c	pertinent to the cathodic reaction
CB	pertinent to the conduction band
eff	effective
H2	pertinent to the hydrogen evolution reaction
i	pertinent to species i
k	pertinent to reaction k
kin	pertinent to the kinetic overpotential
l	pertinent to the limiting current density
mt	pertinent to the mass-transfer overpotential
n	pertinent to the n^{th} light absorber
O	pertinent to the oxidized species
op	pertinent to the operating point of the system
p	pertinent to particle (material, wavelength, and size-dependent properties)
rr	pertinent to the equilibrium radiative recombination current density
R	pertinent to the reduced species
RS	pertinent to the redox shuttle reaction
sc	pertinent to the short-circuit photocurrent density
suspension	suspension
total	total
VB	pertinent to the valence band

Other	
AM1.5	air mass 1.5 reference spectrum for terrestrial solar insolation
H2	hydrogen reaction
NHE	Normal Hydrogen Electrode, used as a reference
RS	pertinent to the redox shuttle reaction
STC	solar-to-chemical efficiency

Photodiode modeling for short-circuit and recombination current densities.

The photodiode behavior for any slab, $n \leq N$, was modeled using the following equation:

$$j = j_{\mathrm{sc},n} - j_{\mathrm{rr}} \left(\exp\left(\frac{q_e \, V}{k_B \, T} \right) - 1 \right) \tag{S1}$$

where, $j_{\mathrm{sc},n}$ is the short-circuit photocurrent density of the n^{th} light absorber, j_{rr} is the equilibrium radiative recombination current density, q_e is the elementary charge, V is the operating potential, k_B is the Boltzmann constant, and T is the temperature. Light absorption per slab, and thus resulting absorptance and incident photon flux for the next slab, is obtained from the Beer-Bouguer-Lambert law,[1] which dictates $j_{\mathrm{sc},n}$,

$$j_{\mathrm{sc},n} = q_e \underbrace{\left(1 - \exp\left(-\frac{\tau_{\mathrm{total}}}{N}\right)\right)}_{\text{absorptance per slab}} \underbrace{\exp\left(-\frac{\tau_{\mathrm{total}}\,(n-1)}{N}\right) \int_{\upsilon_{bg}}^{\infty} \phi_{\mathrm{AM1.5}}(\upsilon)\mathrm{d}\upsilon}_{\text{position dependent incident flux}} \tag{S2}$$

where $\upsilon_{\mathrm{bg}} = E_{\mathrm{bg}} \,/\, k_B \, T$ is the photon frequency based on the bandgap, E_{bg}, of the photodiode, ϕ_{solar} is the incident photon flux, τ_{total} is the total non-dimensional optical thickness, N is the total number of light absorbers modeled, and $n \in [1, N]$ represents the spatial position of the different light absorbers moving from the top to the bottom for $n = 1$ to $n = N$. The total absorptance, A_{total}, was set equal to 0.99, irrespective of the number of light absorbers, which leads to a total optical thickness defined by the following equation:

$$\tau_{\mathrm{total}} = -\ln(1 - A_{\mathrm{total}}) = 4.61 \tag{S3}$$

For the case with multiple light absorbers, i.e., $N > 1$, the optical thickness of an individual light absorber/slab, τ, is,

$$\tau = \frac{\tau_{\mathrm{total}}}{N} \tag{S4}$$

The baseline value of equilibrium radiative recombination current density, j_{rr}, used for most of our calculations (Figures 4-8) is obtained based on: the thermal emission from both top and bottom surfaces of a planar slab light absorber at T to the surroundings; considering re-absorption of emitted photons inside the planar slabs with the same per-slab optical absorptance that was used in Eq. S2; being consistent with the Shockley-Queisser detailed balance model.[2]

$$j_{\mathrm{rr}} = \underbrace{2}_{\substack{\text{top and bottom} \\ \text{emission}}} \underbrace{\left(1 - \exp\left(-\frac{\tau_{\mathrm{total}}}{N}\right)\right)}_{\text{absorptance per slab}} q_e \underbrace{\left(\frac{2\pi}{\mathrm{c}^2}\right) \int_{\upsilon_{bg}}^{\infty} \frac{\upsilon^2}{e^{\frac{h\,\upsilon}{k_{\mathrm{B}}\,T}} - 1} \, \mathrm{d}\upsilon}_{\text{blackbody emission spectrum}} \tag{S5}$$

where, c is the speed of light in vacuum and h is the Planck constant.

Based on Eq. (S2), as the number of light absorbers increases from the case of a single light absorber ($N = 1$) to multiple light absorbers ($N > 1$), the short-circuit photocurrent produced per light absorber, $j_{\mathrm{sc},n}$, decreases, even though the total absorptance, A_{total}, of the ensemble is constant at 0.99. Similarly, the radiative recombination current density in Eq. (S5) decreases per light absorber from a single to multiple light absorbers. Because the open-circuit potential depends on the logarithm of the ratio of the short-circuit photocurrent to the equilibrium recombination currents, it does not change significantly from light absorber to light absorber whether we have one or many light absorbers i.e. for 900 light absorbers, the V_{oc} decreases by less than 10% from

n = 1 to n = 1000. Thus, if a fixed V_{oc} was implemented instead, the studied trends should still hold, even if the magnitude and optimal number of light absorbers might shift. A fixed V_{oc} would result from assuming inter-absorber photon recycling, which has been comprehensively implemented in other work.[3,4]

To further probe influences of recombination rates on the predicted behavior, especially with multiple light absorbers, we also performed analyses with other modeled values (Figure S1) including:

$$j_{rr,max} = 2 \underbrace{\frac{\tau_{total}}{N}}_{\substack{\text{optical thickness} \\ \text{per light absorber/slab}}} q_e \left(\frac{2\pi}{c^2}\right) \int_{\upsilon_{bg}}^{\infty} \frac{\upsilon^2}{e^{\frac{h\upsilon}{k_B T}} - 1} \, d\upsilon \quad \text{(S6)}$$

- a maximum limit for the equilibrium radiative recombination current density, $j_{rr,max}$, based on assuming homogenous emission and no attenuation/absorption of radiative intensity within the volume of the semiconductor slab. This leads to a scaling factor that is just the optical thickness of individual light absorbers, τ_{total} / N, instead of scaling with the absorptance term as in Eq. (S5)[5,6,7]
- recombination currents that are significantly larger than equilibrium radiative recombination currents by several orders of magnitude to emulate physical scenarios where other mechanisms for recombination occur in parallel and are often more dominant that radiative recombination alone, such as trap-assisted recombination.[8,9,10] For these cases, we modeled $j_{rr} = Cj_{rr}$ where C = 10, 100, and 1000.

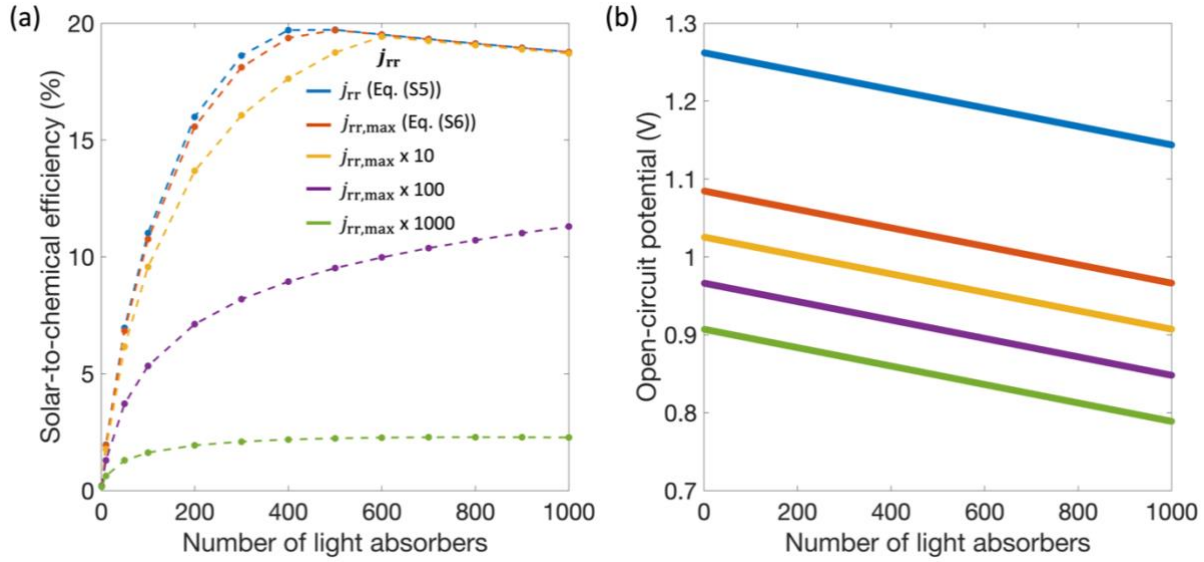

Figure S1: (a) STC efficiencies for an increasing number of light absorbers for different j_{rr} assumptions. (b) Open-circuit potential with respect to light absorber number when N = 900. The additional limiting current densities assumed were: $g_{l,VB} = j_{l,H2,a}$ / $j_{l,RS,a}$ = 1e-2, $g_{l,CB} = |j_{l,RS,c}|$ / $j_{l,RS,a}$ = 1e-2, and $j_{l,H2,c}$ / j_{sc} = -1000. The redox shuttle pair was assumed to be Fe(III)/Fe(II) with redox kinetics parameters of $j_{0,RS}$ = 10 A m^{-2} and $\alpha_{a,RS}$ = 0.5. RS: redox shuttle reaction. H2: hydrogen reaction. For reference, 1 A m^{-2} = 0.1 mA cm^{-2}.

Mass-transfer-limited Butler-Volmer kinetics modeling

Mass-transfer-limited Butler-Volmer kinetics is modeled using:

$$j = j_0 \underbrace{\left(1 - \frac{j}{j_{l,a}}\right)^{\nu_R \, \alpha_c / n_e}}_{C_{s,R}} \underbrace{\left(1 - \frac{j}{j_{l,c}}\right)^{\nu_O \, \alpha_a / n_e}}_{C_{s,O}} \left(\exp\left(\frac{\alpha_a \, \eta_{\text{kin}}}{R \, T/F}\right) - \exp\left(\frac{-\alpha_c \, \eta_{\text{kin}}}{R \, T/F}\right)\right) \tag{S7}$$

Where, j is the current density, j_0 is the exchange current density, $j_{l,a/c}$ are the parametrized anodic (a) and cathodic (c) limiting current densities, $\nu_{R/O}$ are the stoichiometric coefficient magnitudes for the reduction (R) and oxidation (O) reactions, $\alpha_{c/a}$ are the charge transfer coefficients, n_e is the number of electrons, η_{kin} is the kinetic overpotential, R is the gas constant, T is the temperature, and F is the Faraday constant. The scaling terms for the exchange current density in this equation represent the surface concentrations of the reduced and the oxidized species, $C_{s,R}$ and $C_{s,O}$, which are interdependent on the operating and limiting current densities. The concentrations were assumed to be fixed at the electrode/electrolyte interface such that the depletion/accumulation of participating species are not updated as the reactions take place.

Governing equalities

The governing current density equality for the operating current density j_{op} of the photodiode is:

$$j_{\text{op}} = j_{\text{VB,RS}} + j_{\text{VB,H2}} = -(j_{\text{CB,RS}} + j_{\text{CB,H2}}) \tag{S8}$$

The governing potential equality for operating potential V_{op} of the photodiode is as follows, where V_{VB} and V_{CB} are the potentials at which the desired and the competing redox reactions occur at the valence and conduction band states.

$$V_{\text{op}} = V_{\text{VB}} - V_{\text{CB}} \tag{S9}$$

Influences of redox shuttle kinetic parameters for $N = 1$

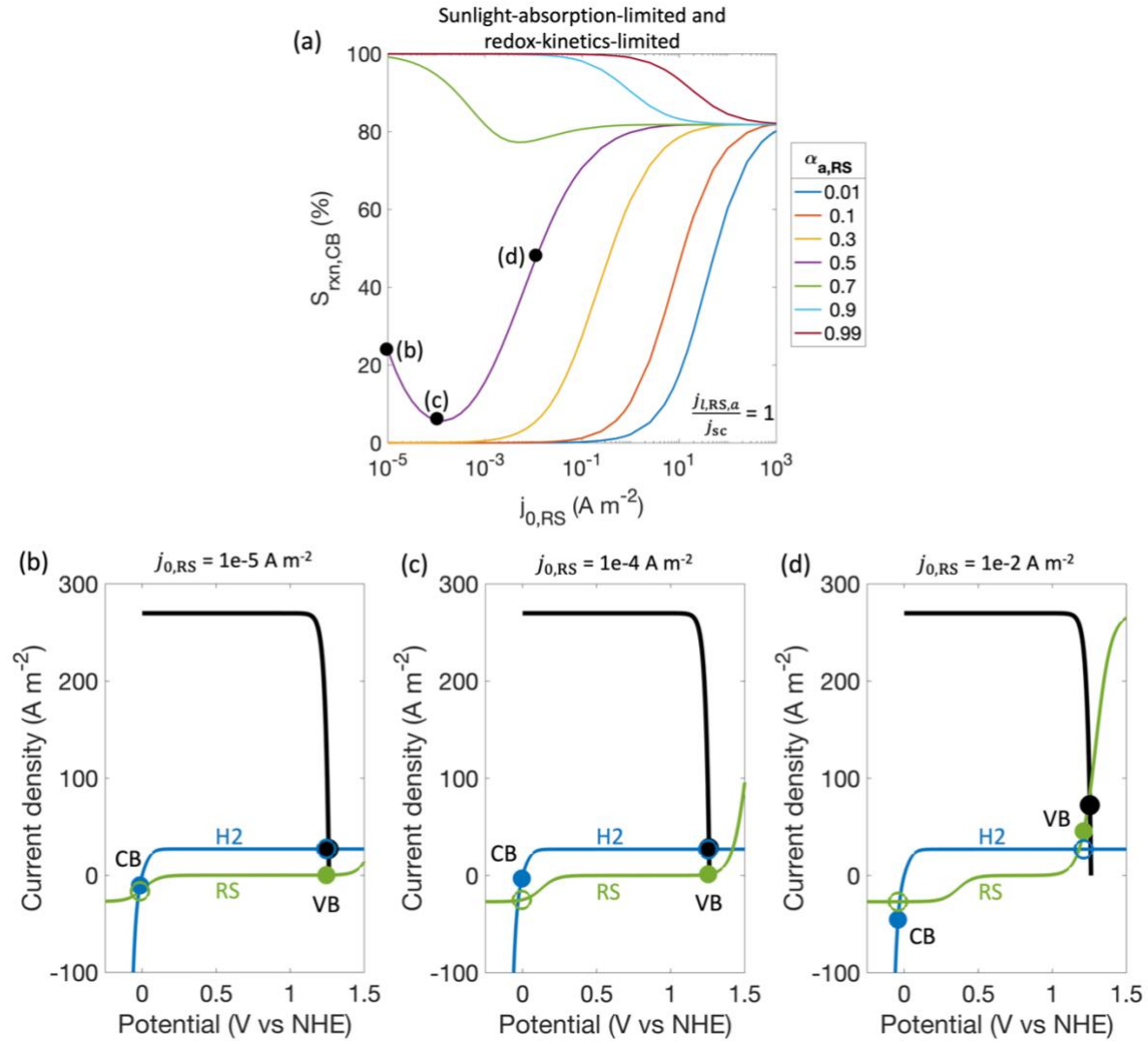

Figure S2: (a) Selectivity (S_{rxn}) toward the desired redox reaction (when competing reactions are implemented) for $j_{l,\text{RS},a}/j_{\text{sc}}$ = 1 at the conduction band (CB) (Figure 4(d)). Load-line analysis depicting photodiode power curve (black), individual reaction load curves (H2: hydrogen reaction in blue, RS: redox shuttle reaction in green), for $\alpha_{a,\text{RS}}$ = 0.5 and (b) $j_{0,\text{RS}}$ = 1e-5 A m^{-2}, (c) $j_{0,\text{RS}}$ = 1e-4 A m^{-2} , and (d) $j_{0,\text{RS}}$ = 1e-2 A m^{-2}. The light absorber was assumed to be optically thick with an absorptance A of 0.99 with a bandgap of 1.55 eV. Other limiting current densities for the competing reactions assumed were based on asymmetry factors, $g_{l,\text{VB}} = j_{l,\text{H2},a} / j_{l,\text{RS},a}$ = 1e-1, $g_{l,\text{CB}} = |j_{l,\text{RS},c}| / j_{l,\text{RS},a}$ = 1e-1; limiting current density for the desired H2 evolution reaction, $j_{l,\text{H2},c} / j_{\text{sc}}$ = -1000; and $j_{l,\text{RS},a}/j_{\text{sc}}$ = 1. The redox shuttle pair assumed here was Fe(III)/Fe(II). RS: redox shuttle reaction. H2: hydrogen reaction.

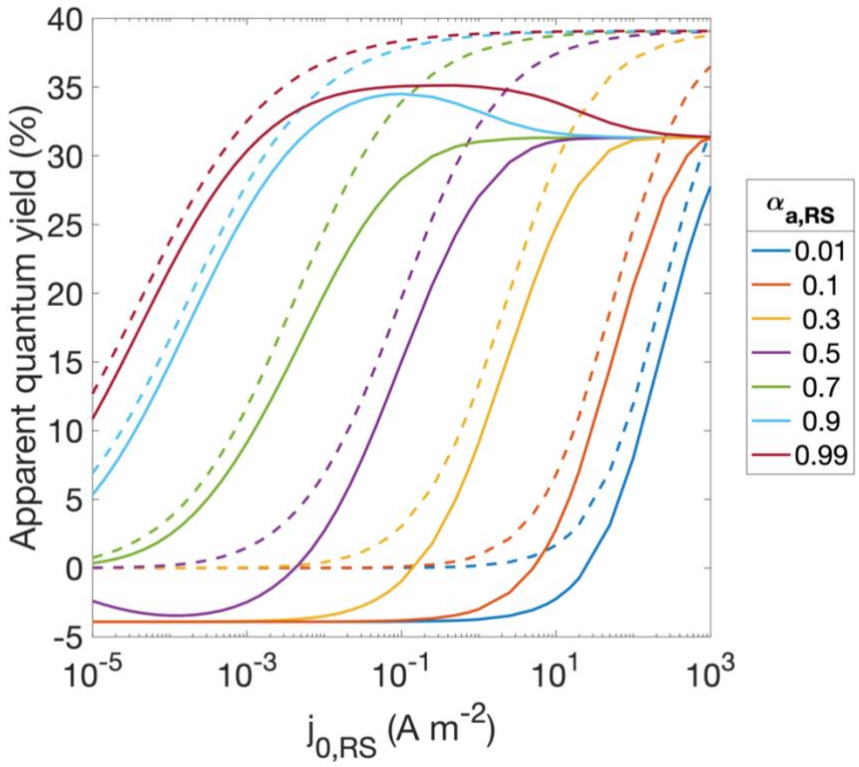

Figure S3: Apparent quantum yield for $j_{l,\mathrm{RS},a}$ / j_{sc} = 1 for selective reactions (dashed lines) and with inclusion of competing reactions (solid lines). A single optically thick (absorptance A of 0.99) light absorber was modeled, N = 1 with a bandgap of 1.55 eV. The additional limiting current densities assumed were: $g_{\mathrm{l,VB}}$ = $j_{l,\mathrm{H2},a}$ / $j_{l,\mathrm{RS},a}$ = 1e-1, $g_{\mathrm{l,CB}}$ = $|j_{l,\mathrm{RS},c}|$ / $j_{l,\mathrm{RS},a}$ = 1e-1, and$j_{l,\mathrm{H2},c}$ / j_{sc} = -1000. The redox shuttle pair was assumed to be Fe(III)/Fe(II). RS: redox shuttle reaction. H2: hydrogen reaction. For reference, 10^{0} A m^{-2} = 10^{-1} mA cm^{-2}.

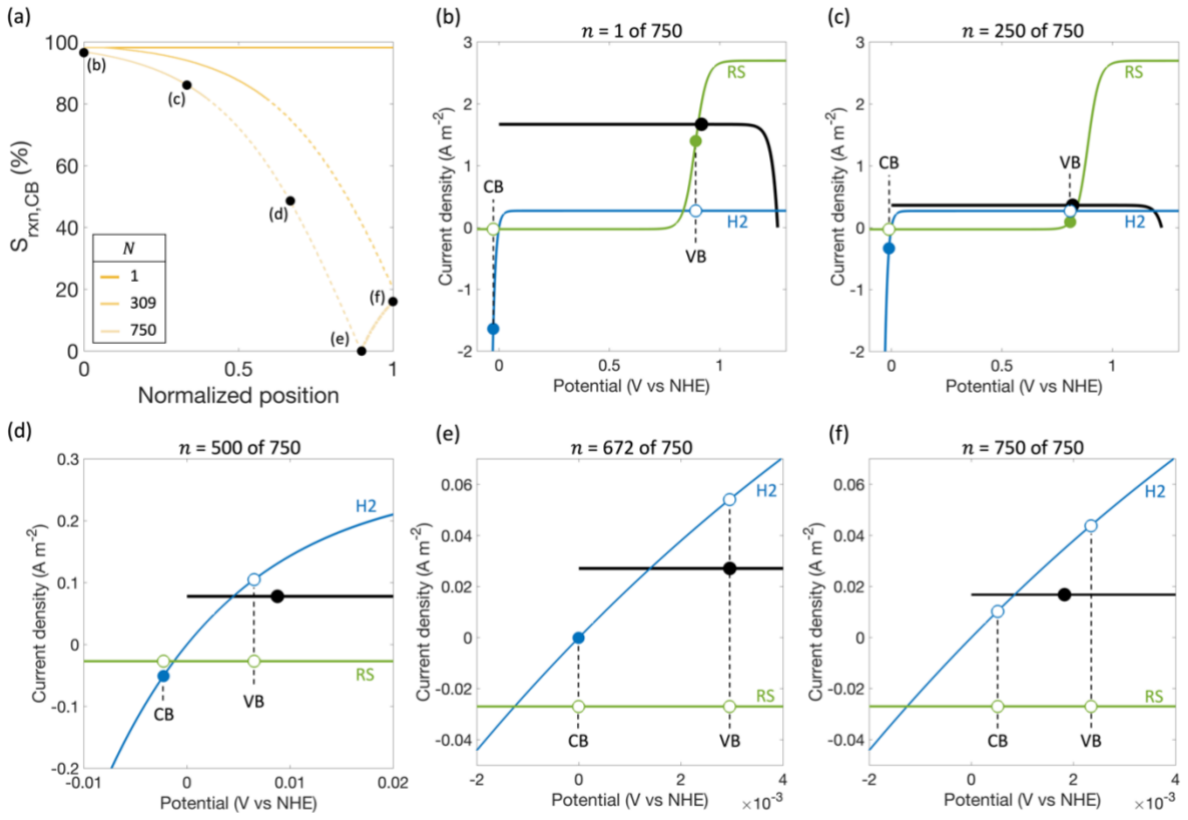

Figure S4: (a) Reaction selectivity S_{rxn} towards the H2 reduction at the conduction band for $g_{l,\mathrm{CB}}$ = 1e-2 with $g_{l,\mathrm{VB}}$ = 1e-4 and different N values. Solid lines indicate desired reactions taking place; dotted lines indicate H_2 oxidation taking place at CB; dashed lines show RS reduction at VB; thick dash-dot lines indicate both undesired reactions (H_2 oxidation and RS reduction) taking place. Load-line analysis depicting photodiode power curve (black), individual reaction load curves (H2: hydrogen reaction in blue, RS: redox shuttle reaction in green), for (a) n = 1 of 750, (b) n = 250 of 750, (c) n = 500 of 750, (d) n = 672 of 750, and (b) n = 750 of 750. Undesired reactions (H_2 oxidation and RS reduction) indicated by the empty markers. For all plots, the light absorber was assumed to be optically thick with an absorptance A of 0.99 with a bandgap of 1.55 eV. Other limiting current densities for the competing reactions assumed were based on asymmetry factors, $g_{l,\mathrm{VB}} = j_{l,\mathrm{H2},a} / j_{l,\mathrm{RS},a}$ = 1e-4, $g_{l,\mathrm{CB}} = |j_{l,\mathrm{RS},c}| / j_{l,\mathrm{RS},a}$ = 1e-2; limiting current density for the desired H2 evolution reaction, $j_{l,\mathrm{H2},c} / j_{\mathrm{sc}}$ = -1000; and $j_{l,\mathrm{RS},a}/j_{\mathrm{sc}}$ = 1e-2. The redox shuttle pair assumed here was Fe(III)/Fe(II) with $j_{0,\mathrm{RS}}$ = 10 A m^{-2} and $\alpha_{a,\mathrm{RS}}$ = 0.5. RS: redox shuttle reaction. H2: hydrogen reaction. CB: conduction band. VB: valence band.

Table S1: Assumed constants and model parameters

Parameter	Value	
Semiconductor and optical properties		
Bandgap E_{bg} (eV)	1.55	
Short-circuit photocurrent density j_{sc} (A m^{-2}) for N = 1	270	
Equilibrium radiative recombination current density j_{rr} (A m^{-2})	using Eq. (S5) 1.24e-19	using Eq. (S6) 5.79e-19
Reaction kinetics		
Reaction k	RS	H2
Standard reduction potential E_{eq} (V *vs* NHE)	0.77, 1, 1.23	0
Reference exchange current density $j_{0,k}$ (A m^{-2})	1e-5 – 1e3	10 [11]
Anodic charge transfer coefficient $\alpha_{a,k}$	0.01 – 0.99	1* [5,6,12]
Electrons exchanged n_e	1, 6, 2	2
Limiting current density ratios		
$j_{l,\mathrm{RS},a}$ / j_{sc}	1e-2, 1	
$\lvert j_{l,\mathrm{RS},c}\rvert$ / $j_{l,\mathrm{RS},a}$	1e-4 – 10	
$j_{l,\mathrm{H2},a}$ / $j_{l,\mathrm{RS},a}$	1e-4 – 10	
$\lvert j_{l,\mathrm{H2},c}\rvert$ / j_{sc}	1000	

*The charge-transfer coefficients for H_2 were assumed to be equal to 1. In the literature, Pt in acidic conditions has been thoroughly studied and is known to have a Tafel slope that is dependent on the applied potential, ranging from 30 mV dec^{-1} at low overpotentials (corresponding to α_a = 2) to 120 mV dec^{-1} at high overpotentials (corresponding to α_a = 0.5). Because this potential dependence was not implemented in our present calculations, and the current–overpotential relationship does not vary significantly when $\alpha_{a,\mathrm{H2}} \geq 1$, $\alpha_{a,\mathrm{H2}} = 1$ was assumed for all cases studied such that perfect theoretical symmetry ($\alpha_{a,\mathrm{H2}} + \alpha_{c,\mathrm{H2}} = n_e = 2$) was always respected. Conway and Bai have also experimentally reported $\alpha_{a,\mathrm{H2}} \sim 1$ for a Pt catalyst using rotating disk electrode measurements.[77]

References

1. T. G. Mayerhöfer, S. Pahlow and J. Popp, *Chemphyschem*, 2020, **21**, 2029–2046.
2. W. Shockley and H. J. Queisser, *J Appl Phys*, 1961, **32**, 510–519.
3. S. T. Keene, "Detailed Balance Modeling of Novel Solar Fuels Designs", University of California, Irvine, 2018.
4. Sam Keene, Gabriel S. Phun, Zejie Chen and Shane Ardo, *Nature Materials (under revision)*, 2024
5. A. Martí, J. L. Balenzategui and R. F. Reyna, *J Appl Phys*, 1997, **82**, 4067–4075.
6. R. Brenes, M. Laitz, J. Jean, D. W. Dequilettes and V. Bulović, *Phys Rev Appl*, 2019, **12**, 014017.
7. A. Braun, E. A. Katz, D. Feuermann, B. M. Kayes and J. M. Gordon, *Energy Environ Sci*, 2013, **6**, 1499–1503.
8. B. Zutter, Z. Chen, L. Barrera, W. Gaieck, A. S. Lapp, K. Watanabe, A. Kudo, D. V. Esposito, R. Bala Chandran, S. Ardo and A. A. Talin, *ACS Nano*, 2023, **17**, 9405–9414.
9. J. Nelson, *The Physics of solar cells*, 2003.
10. P. Würfel, *Physics of solar cells: From Principles to New Concepts*, 2005.
11. S. Trasatti, *J Electroanal Chem Interfacial Electrochem*, 1972, **39**, 163–184.
12. J. Newman and K. E. Thomas-Alyea, *Electrochemical Systems*, 3rd edn., 2004.